Turbulent cascade arrests and the formation of intermediate-scale condensates

Kolluru Venkata Kiran,[1] Dario Vincenzi,[2] and Rahul Pandit[1]
[1] *Centre for Condensed Matter Theory, Department of Physics, Indian Institute of Science, Bangalore, 560012, India*
[2] *Université Côte d'Azur, CNRS, LJAD, 06100 Nice, France*
(Dated: April 10, 2024)

Energy cascades lie at the heart of the dynamics of turbulent flows. In a recent study of turbulence in fluids with odd-viscosity [de Wit *et al.*, Nature **627**, 515 (2024)], the two-dimensionalization of the flow at small scales leads to the arrest of the energy cascade and selection of an intermediate scale, between the forcing and the viscous scales. To investigate the generality of this phenomenon, we study a shell model that is carefully constructed to have three-dimensional turbulent dynamics at small wavenumbers and two-dimensional turbulent dynamics at large wavenumbers. The large scale separation that we can achieve in our shell model allows us to examine clearly the interplay between these dynamics, which leads to an arrest of the energy cascade at a transitional wavenumber and an associated accumulation of energy at the same scale. Such pile-up of energy around the transitional wavenumber is reminiscent of the formation of condensates in two-dimensional turbulence, *but, in contrast, it occurs at intermediate wavenumbers instead of the smallest wavenumber.*

Introduction. Cascade processes are at the origin of the multiscale nature of turbulent flows. The best-known example is Richardson's cascade of kinetic energy in three dimensions (3D) [1]. Energy is injected into a characteristic wavenumber k_f by an external force that drives the flow. On average, nonlinear interactions transfer the injected energy to larger wavenumbers k without dissipation. This process persists up to the Kolmogorov wavenumber, beyond which viscous dissipation dominates. The continuous interplay between energy injection and viscous dissipation leads to a non-equilibrium statistically stationary state. The direct energy cascade is at the heart of 3D homogeneous isotropic turbulence [1]. In two-dimensional (2D) turbulence, the direction of the energy cascade is reversed, and on average energy flows from k_f to smaller values of k; furthermore, the inverse cascade of energy coexists with a direct cascade of enstrophy [2, 3]. In general, turbulent cascades of inviscid invariants, and in particular their directions (whether direct or inverse), are affected by phenomena such as rotation, stratification, spatial confinement, and selective suppression of Fourier modes of the velocity [4–7].

Dissipative mechanisms inherent to the system, typically viscous dissipation at large k or frictional dissipation at small k, naturally arrest or suppress a turbulent cascade. However, other complex mechanisms can induce such suppression. For example, a recent study [8] of an instability-mediated forcing in a 2D fluid has shown the suppression of the inverse energy cascade via the accumulation of energy at the forcing wavenumbers and, consequently, the formation of coherent vortices at those scales. In magnetohydrodynamic (MHD) turbulence, the energy cascade is suppressed when the flow is subjected to a large-scale background magnetic field along with a strong rotation that is not aligned with it [9]. In bacterial turbulence, the inverse energy cascade gets suppressed as bacterial activity decreases [10, 11]. Recently, de Wit *et al.* [12] have studied the 3D Navier–Stokes equations (NSE) with an odd-viscosity term that is proportional to the Laplacian of the velocity and oriented in a fixed direction. This term leads to a quasi-two-dimensionalization of the velocity field at large k. Two cases arise. If the forcing acts at small k, the direct energy cascade is arrested at a critical wavenumber k_c. Since odd viscous terms are not dissipative, the arrest of the cascade results in an accumulation (or "condensation") of energy around k_c and thence an emergence of flow structures of size k_c^{-1}. If the flow is forced at large wavenumbers, this model displays an inverse energy cascade, which is arrested by the 3D-type behavior of the flow at small k and is again accompanied by the formation of spatial structures of intermediate sizes.

We extend the investigation of turbulent systems where 3D-type dynamics, at small k, coexist with 2D-type dynamics, at large k. To address this problem in sufficient generality and with enough wavenumber resolution, we construct a shell model that can display the desired small- and large-k dynamics. Shell models are a class of dynamical equations, which resemble the NSE in Fourier space and offer insights into energy-transfer mechanisms in fully developed turbulence [1, 13–16]. The interactions between the Fourier modes of the velocity are restricted; thus, numerical simulations of shell models reach larger scale separations and better statistical convergence than those presently achievable with direct numerical simulations of the NSE [17]. The tractability of shell models makes them invaluable for studying turbulence. New concepts in turbulence theory that have been recently developed by using shell models include hidden scale invariance [18], subgrid closures [19], stirring strategies for optimizing mixing [20], and the application of avalanche dynamics in amorphous materials in the analysis of the temporal behavior of the kinetic energy [21]. We follow the strategy that was used by

Boffetta *et al.* [22] for a shell-model study of thin fluid layers. By allowing the coefficients of the shell model to depend suitably on k, the model captured the split-energy-cascade, in quasi-2D turbulent flows, with direct and inverse components [23, 24]. We also consider scale-dependent coefficients but select them so as to obtain a shell model that is 3D-like at small wavenumbers and 2D-like at large wavenumbers. The transition between the two cascading regions occurs at a wavenumber $k_{\rm tr}$; the forcing is localized at the wavenumber k_f. We find that, irrespective of the ratio of $k_{\rm tr}/k_f$, the reciprocity between the small- and large-wavenumber dynamics results in the arrest of the energy cascade (be it forward or inverse). However, the system dynamics differs depending on whether $k_{\rm tr}/k_f$ is smaller or greater than unity. The main consequence of the arrest of the cascade is a strong build-up of energy close to $k_{\rm tr}$. We show that a statistically stationary state is nevertheless possible because of an increase in viscous dissipation near $k_{\rm tr}$.

Model. We consider the SABRA shell model [25, 26]

$$\frac{du_n}{dt} = \mathrm{i}\Phi_n - (\mu k_n^{-2} + \nu k_n^2)u_n + f_n, \quad 1 \le n \le N, \quad (1)$$

where $k_n = k_0\lambda^n$, μ and ν are the hyper-friction and viscosity parameters, respectively, and the external forcing, $f_n = \epsilon_f(1+\mathrm{i})\delta_{n,n_f}/2u^*_{n_f}$, injects energy at a constant rate ϵ_f into the shell n_f. The nonlinear term is

$$\begin{aligned}\Phi_n &= a_n k_{n+1} u_{n+2} u^*_{n+1} + b_n k_n u_{n+1} u^*_{n-1} \\ &- c_n k_{n-1} u_{n-2} u_{n-1}, \end{aligned} \quad (2)$$

where a_n, b_n, c_n are real and the $*$ denotes complex conjugation. In addition, $u_{-1} = u_0 = u_{N+1} = u_{N+2} = 0$. In the inviscid ($\mu = 0$, $\nu = 0$) and unforced ($f_n = 0$) case, the total energy $E(t) = \frac{1}{2}\sum_{n=1}^{N} |u_n(t)|^2$ is conserved provided $a_{n-1} + b_n + c_{n+1} = 0$. In the original SABRA model [25], $a_n = a$, $b_n = b$, and $c_n = c$, and $H(t) = \frac{1}{2}\sum_{n=1}^{N} (a/c)^n |u_n(t)|^2$ is a second invariant quantity. Different regimes are observed depending on the ratio c/a. Here, it is sufficient to recall that there is a regime of direct energy cascade, which mimics 3D turbulence, for $-1 < c/a < 0$ [25]. In this regime, H does not have a definite sign and it can be regarded as a generalized helicity. By contrast, H is positive for $0 < c/a < 1$, and in the subrange $\lambda^{-2/3} < c/a < 1$ there is a 2D-turbulence-like regime, with a simultaneous inverse cascade of E and a direct cascade of H, where H plays the role of a generalized enstrophy [26].

To introduce a shell-model analog of the domain aspect ratio in a study of quasi-2D fluid turbulence, Ref. [22] considered a version of the SABRA model with n-dependent coefficients: $\{a_n, b_n, c_n\}$ were chosen to generate an inverse energy cascade for $k_n < k_h$ and a direct energy cascade for $k_n > k_h$, with k_h^{-1} representing the depth of a fluid layer.

Run	N	n_f	$n_{\rm tr}$	ν	μ	δt
A0	28	1	∞	5×10^{-7}	0	1×10^{-4}
A1	28	1	25	5×10^{-7}	0	1×10^{-4}
A2	28	1	20	5×10^{-7}	0	1×10^{-4}
A3	28	1	18	5×10^{-7}	0	1×10^{-4}
A4	28	1	15	5×10^{-7}	0	1×10^{-4}
A5	28	1	12	5×10^{-7}	0	1×10^{-4}
A6	28	1	10	5×10^{-7}	0	5×10^{-5}
B1	28	1	15	1×10^{-7}	0	1×10^{-4}
B2	28	1	15	1×10^{-8}	0	1×10^{-5}
B3	28	1	15	5×10^{-9}	0	1×10^{-5}
C1	34	3	5	1×10^{-10}	1×10^{-3}	1×10^{-4}
C2	34	3	7	1×10^{-10}	1×10^{-3}	1×10^{-4}
C3	34	3	9	1×10^{-10}	1×10^{-3}	1×10^{-4}
D1	34	25	0	1×10^{-10}	5×10^{-4}	1×10^{-5}
D2	34	25	15	1×10^{-10}	5×10^{-4}	1×10^{-6}
D3	34	25	17	1×10^{-10}	5×10^{-4}	1×10^{-6}
D4	34	25	18	1×10^{-10}	5×10^{-4}	1×10^{-6}
D5	34	25	20	1×10^{-10}	5×10^{-4}	1×10^{-6}

TABLE I. Parameters of the shell-model simulations. In addition, $\lambda = 2$, $k_0 = 1/16$, and $\epsilon_f = 5\times10^{-3}$ for all runs.

We also consider a shell model with n-dependent coefficients *but reverse the directions of the energy cascades* by taking

$$a_n = 1,\ b_n = -0.5,\ c_n = -0.5, \quad 1 \le n < n_{\rm tr}\,, \quad (3)$$

$$a_n = 1,\ b_n = -1.7,\ c_n = -0.5, \quad n = n_{\rm tr}\,, \quad (4)$$

$$a_n = 1,\ b_n = -1.7,\ c_n = 0.7, \quad n_{\rm tr} < n \le N\,. \quad (5)$$

Clearly, for modes $n < n_{\rm tr}$ ($n > n_{\rm tr}$) the coefficients $\{a_n, b_n, c_n\}$ lead to a 3D (2D) turbulent-like regime. Note that c_n changes value at $n_{\rm tr+1}$ to respect energy conservation in the inviscid limit. We investigate the interplay between the small- and large-k_n modes in this model for the cases (a) $k_{\rm tr}/k_f > 1$ and (b) $k_{\rm tr}/k_f < 1$, with $k_{\rm tr} = k_0\lambda^{n_{\rm tr}}$ the transitional wavenumber. We integrate Eq. (1) by using an Adams-Bashforth scheme [27].

(a) Small-wavenumber forcing. We first consider the case $k_f < k_{\rm tr}$ (Table I, runs A and B, in which $\mu = 0$). In the limit $k_{\rm tr}/k_f \to \infty$, we recover the SABRA model with constant 3D-like coefficients; therefore, in this limit, our model displays a direct cascade of E [25]; and the energy flux [$\langle\cdot\rangle$ is the time average]

$$\Pi_E(k_n) = \left\langle \sum_{j=n}^{N} \Re\{\Phi_j u_j^*\} \right\rangle \quad (6)$$

is constant and equal to ϵ_f for $k_f \ll k_n \ll k_\nu$, where $k_\nu = (\epsilon_f/\nu^3)^{1/4}$ is the Kolmogorov wavenumber. In the same range, the energy spectrum $\mathcal{E}(k_n) = \langle |u_n|^2/k_n\rangle$ shows a scaling range that is consistent with $k_n^{-5/3}$, the

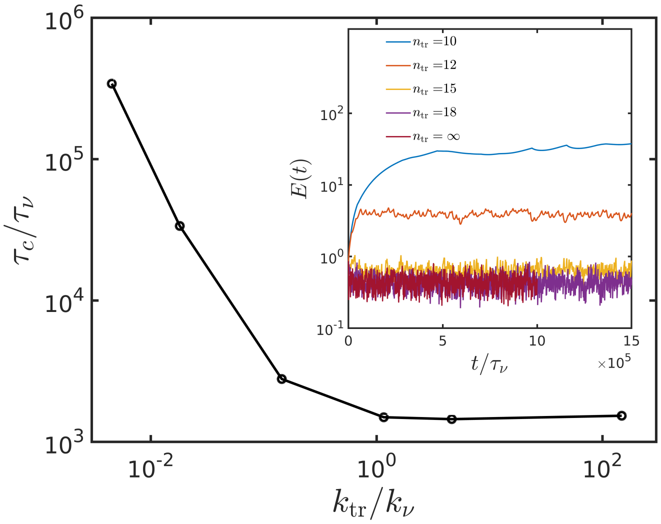

FIG. 1. Plot of the energy-autocorrelation decay time τ_c, scaled by the Kolmogorov time $\tau_\nu = \sqrt{\nu/\epsilon_f}$, as a function of $k_{\rm tr}/k_\nu$. Inset: the time series of the total energy for different values of $n_{\rm tr}$ (runs A0, A3, A4, A5, and A6).

Kolmogorov (1941) form [1]. For $k_n \ll k_f$, $\mathcal{E}(k_n) \sim k_n^{-1}$, which indicates energy equipartition [5]. Now consider $1 < k_{\rm tr}/k_f \ll \infty$. If $k_{\rm tr} \gtrsim k_\nu$, $E(t)$ does not show significant deviations from the limiting case $k_{\rm tr}/k_f \to \infty$ [inset of Fig. 1]. However, when $k_{\rm tr} < k_\nu$ we find that, with decreasing $k_{\rm tr}$ (and fixed k_f), $E(t)$ takes longer to reach the stationary state, and its stationary value increases [inset of Fig. 1]. To characterize the temporal energy fluctuations $E'(t) = E(t) - \langle E(t)\rangle$ for different $k_{\rm tr}$, we calculate the time scale τ_c from the exponential decay of the autocorrelation function $C(\tau) = \langle E'(t+\tau)E'(t)\rangle / \langle E'^2(t)\rangle$. Figure 1 shows that τ_c is nearly independent of $k_{\rm tr}$, for $k_{\rm tr} \geq k_\nu$, but it grows rapidly as $k_{\rm tr}$ is decreased below k_ν. These trends are reminiscent of the formation of large-scale condensates in 2D turbulent flows [2, 28], where, in the absence of friction, condensate formation is associated with very long saturation times and strong deviations of the energy spectrum from its inertial-range scaling [compare Fig. 2 of Ref. [28] with our Fig. 1]. Therefore, we examine the dependence of energy spectra and flux on $k_{\rm tr}$. In Fig. 2(a), we plot $\Pi_E(k_n)$ [Eq.(6)] for different values of $k_{\rm tr}$. As long as $k_{\rm tr} > k_\nu$, this flux is indistinguishable from that of the $k_{\rm tr}/k_f \to \infty$ case. However, if $k_{\rm tr} < k_\nu$, $\Pi_E(k_n) \simeq \epsilon_f$ only for $k_f < k_n < k_{\rm tr}$, and it vanishes rapidly beyond $k_{\rm tr}$. Thus, the direct energy cascade persists up until $k_{\rm tr}$, but is then arrested by the 2D-like dynamics for $k_n > k_{\rm tr}$. The consequence of this arrest is a sharp build-up of energy around $k_{\rm tr}$, as seen in Fig. 2(b), where we plot the compensated energy spectra $k_n^{5/3}\mathcal{E}(k_n)$ versus $k_n/k_{\rm tr}$, for different values of $k_{\rm tr}$. Energy starts accumulating around $k_{\rm tr}$ for $k_{\rm tr} < k_\nu$; this accumulation increases as $k_{\rm tr}$ approaches k_f. We also remark that the suppression of high-frequency fluctuations in $E(t)$, with decreasing $k_{\rm tr}$, is associated with the arrest of the energy cascade at $k_n \approx k_{\rm tr}$. Despite the build up of energy at a scale smaller than k_ν, our model reaches a statistically stationary state, albeit at times that increase as $k_{\rm tr}$ decreases. To understand this intriguing behavior, we examine the energy budget in the statistically stationary state:

$$T(k_n) + D_\mu(k_n) + D_\nu(k_n) + F(k_n) = 0\,; \qquad (7)$$

$T(k_n) = \langle \Re\{\Phi_n u_n^*\}\rangle$, $F(k_n) = \langle \Re\{f_n u_n^*\}\rangle$, $D_\nu(k_n) = \langle 2\nu k_n^2 |u_n|^2\rangle$, and $D_\mu(k_n) = \langle 2\mu k_n^{-2}|u_n|^2\rangle$, are the nonlinear, forcing, viscous, and friction contributions, respectively, which we plot in the inset of Fig. 2(c) for $n_{\rm tr} = 10$.

Since friction is absent, the forcing term is balanced by the transfer term at $k_n = k_f$, and, in the cascade range $k_n < k_{\rm tr}$, the contribution from the transfer term is negligible, so the statistical properties are like those in the pure 3D direct cascade ($k_{\rm tr}/k_f \to \infty$). Deviations from this 3D cascade arise when we account for the dissipation term. The maximum of $|D_\nu(k_n)|$ shifts from $k_n \simeq k_\nu$ to $k_n \simeq k_{\rm tr}$, thus compensating for the accumulation of energy at the same wavenumbers, as we show in the inset of Fig. 2(c), where $T(k_n)$ is balanced by $D_\nu(k_n)$ at $k_n \simeq k_{\rm tr}$. Moreover, as $k_{\rm tr}$ decreases, the maximum of $|D_\nu(k_n)|$ shifts to smaller values of k_n and its magnitude increases to compensate for the stronger build-up of energy [Fig. 2(c)].

In the range $k_n > k_{\rm tr}$, the coefficients in Eq. (3) lead to 2D-like dynamics; hence, $H(t)$ is both positive definite and conserved locally. By analogy with the inverse-cascade regime in 2D fluid turbulence, we expect that the energy that accumulates at $k_n \simeq k_{\rm tr}$ acts as a source for the direct cascade of H in the range $k_{\rm tr} \ll k_n \ll k_\nu$. To confirm this, we plot, in Fig. 3(a), the flux of H:

$$\Pi_H(k_n) = \left\langle \sum_{j=n}^{N} \Re\left\{k_n^\beta \Phi_j u_j^*\right\}\right\rangle, \qquad (8)$$

where $\beta = \log_\lambda(a/c)$. Clearly, as $k_{\rm tr}$ is decreased, the flux increases and tends to flatten for $k_{\rm tr} \ll k_n \ll k_\nu$, suggesting a direct cascade of H. However, the lack of significant separation between $k_{\rm tr}$ and k_ν makes it difficult to identify a range where $\Pi_H(k_n)$ remains constant. In the inset of Fig. 3(a), we plot $\Pi_H(k_n)$ for fixed $k_{\rm tr}$ and different values of ν to observe indeed that, for small viscosities, $\Pi_H(k_n)$ tends to flatten for $k_{\rm tr} \ll k_n \ll k_\nu$.

As further confirmation of the direct cascade of H, we show in Fig. 3(b) that, by moving $k_{\rm tr}$ close to k_1, we achieve a large range of constant $\Pi_H(k_n)$, in which $\mathcal{E}(k_n) \sim k_n^{-\gamma}$ with $\gamma = 2[1+\beta]/3 + 1$ [inset of Fig. 3(b)], as is expected in the direct-cascade regime of H [26].

(b) Large-wavenumber forcing. We now address the case $k_f > k_{\rm tr}$ [Table I, runs D; $\mu \neq 0$ helps the system to reach a statistically stationary state]. For $k_{\rm tr} = 0$ and with our choice of parameters, $\mathcal{E}(k_n) \sim k_n^{-5/3}$, in

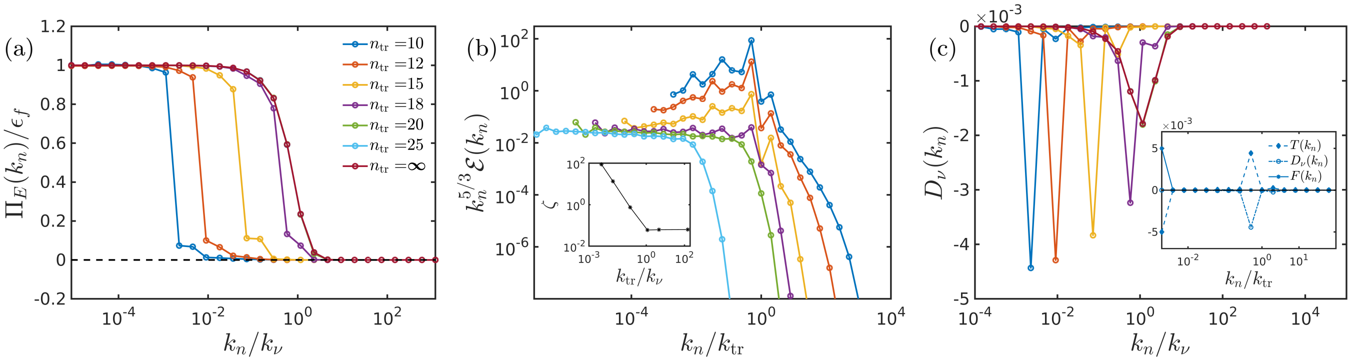

FIG. 2. (a) Log-linear plot of the scaled energy flux versus k_n/k_ν for different values of $n_{\rm tr}$ (runs A0 to A6); the plots for $n_{\rm tr}=20,25$ are indistinguishable from the $n_{\rm tr}=\infty$ curve. (b) Log-log plots of the compensated energy spectra versus $k_n/k_{\rm tr}$ for the values of $n_{\rm tr}$ in (a) [$k_{\rm tr}=k_0\lambda^{n_{\rm tr}}$]; inset: the value of the peak ζ of the compensated spectrum versus $k_{\rm tr}/k_\nu$. (c) Log-linear plot of $D_\nu(k_n)$ versus k_n/k_ν for different values of $n_{\rm tr}$ (runs A); the plots for $n_{\rm tr}=20,25$ are indistinguishable from the $n_{\rm tr}=\infty$ curve; inset: log-linear plots of $T(k_n)$, $D_\nu(k_n)$, and $F(k_n)$ versus k_n/k_ν for the representative value $n_{\rm tr}=10$. The color coding for $n_{\rm tr}$ is the same in (a)-(c).

the range between the friction-dominated wavenumbers and k_f [26]. In this range, $\Pi_E(k_n)<0$ remains constant and equals the rate of hyper-friction energy dissipation $\epsilon_\mu=\sum_{n=1}^{N}D_\mu(k_n)$.

We now consider $k_f>k_{\rm tr}>0$. Small values of $k_{\rm tr}$ have a negligible effects on energy spectra and fluxes, because at small k_n the inverse energy cascade is already stopped by hyper-friction; so we focus on intermediate values of $k_{\rm tr}$ between k_1 and k_f, where the energy flux [Fig. 4(a)] indicates that the inverse energy cascade is arrested at $k_n\simeq k_{\rm tr}$ and it is accompanied by energy build-up around $k_{\rm tr}$ [Fig. 4(b)].

We see the following two scaling forms on each side of $k_{\rm tr}$: For $k_1\ll k_n\ll k_{tr}$, $\mathcal{E}(k_n)\sim k_n^{-1}$, which indicates equipartition [Fig. 4(b)]; and for $k_{\rm tr}\ll k_n\ll k_f$, $\mathcal{E}(k_n)\sim k_n^{-5/3}$, as we expect in the range of the inverse energy cascade [inset of Fig. 4(b)]. Clearly, the latter range decreases as $k_{\rm tr}$ approaches k_f. The energy transfer that leads to a statistically stationary state is similar to that observed in case (a): the accumulation of energy at scales comparable to $k_{\rm tr}$ is compensated by an increased viscous dissipation at similar scales. Indeed, in Fig. 4(a) we see, together with a peak of dissipation at k_f, a second peak at $k_{\rm tr}$ [29].

Our study sheds new light on a general energy-transfer mechanism for the non-dissipative arrest of energy cascades (inverse or direct) when 3D turbulent dynamics, at small k, coexists with 2D turbulent dynamics, at large k. The shell-model approach we employ allows us to cover a large range of wavenumbers; this is crucial for uncovering the subtle interplay between the nonlinear and viscous terms. Specifically, we find that, when $k_{\rm tr}/k_f>1$, the direct energy cascade for $k_n<k_{\rm tr}$ is arrested by the 2D-like dynamics at $k_n>k_{\rm tr}$. In contrast, when $k_{\rm tr}/k_f<1$, the inverse energy cascade for $k_n>k_{\rm tr}$ is arrested by the 3D-like dynamics at $k_n<k_{\rm tr}$. In both cases, the arrest

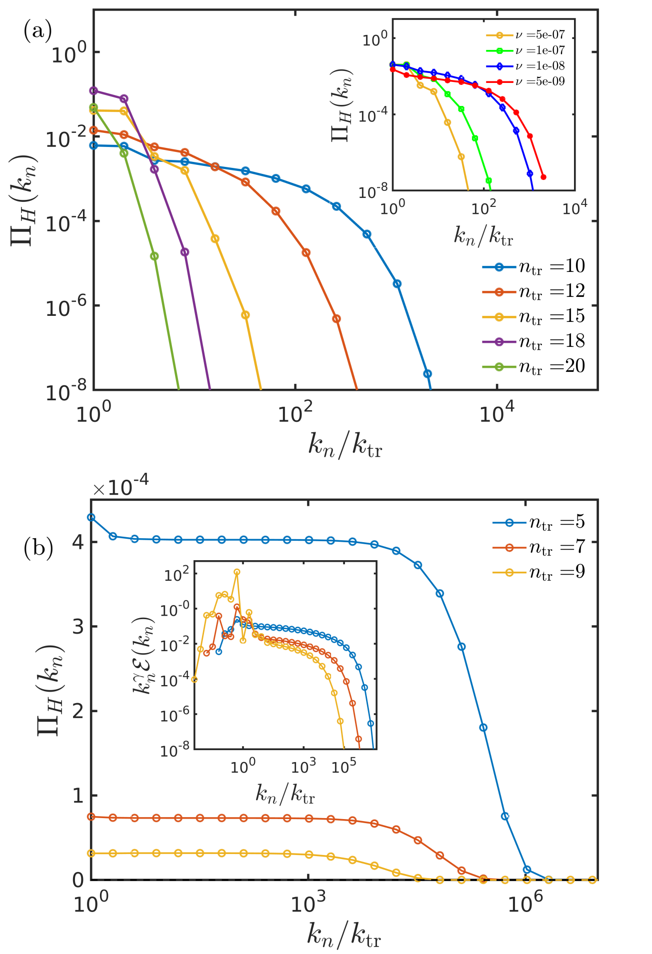

FIG. 3. Log-linear plots of (a) $\Pi_H(k_n)$ versus $k_n/k_{\rm tr}$ for runs A1-A6 and, in the inset, for runs A6, B1, B2 and B3, and (b) for runs C1-C3. Inset of (b): log-log plots of compensated energy spectra versus $k_n/k_{\rm tr}$.

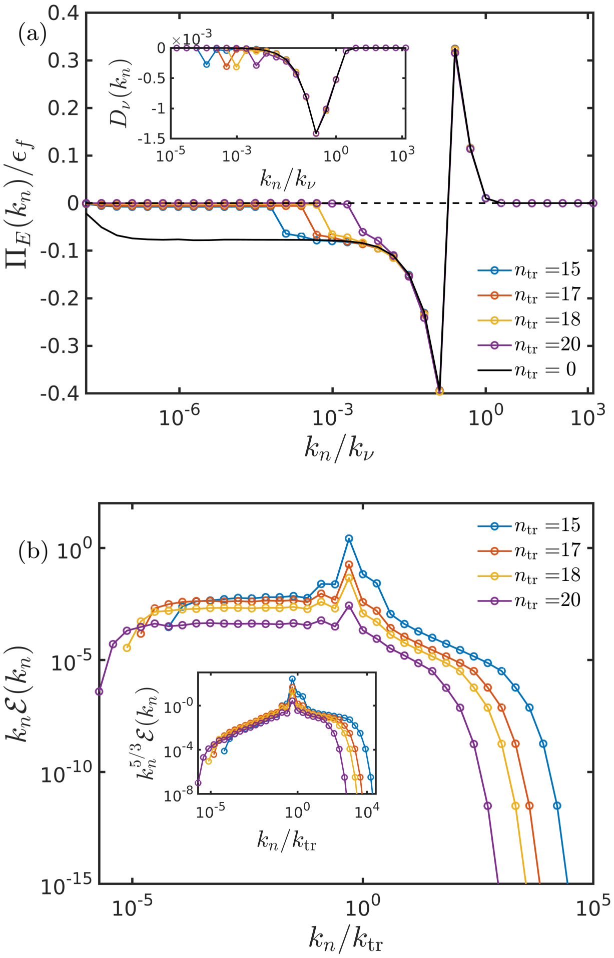

FIG. 4. Plots for runs D1-D5: (a) Log-log plot of the compensated spectra $k_n \mathcal{E}(k_n)$ versus $k_n/k_{\rm tr}$ and in the inset the compensated spectra $k_n^{5/3}\mathcal{E}(k_n)$ versus $k_n/k_{\rm tr}$. (b) Log-linear plots of $\Pi(k_n)$ versus k_n/k_ν and in the inset $D_\nu(k_n)$ versus k_n/k_ν.

of the cascade, close to $k_{\rm tr}$, results in energy accumulation around $k_{\rm tr}$. In a spatially extended system, such an accumulation of energy would lead to the emergence of spatial structures, or condensates, of size $k_{\rm tr}^{-1}$. A statistically stationary state stems from an increased viscous dissipation, at wavenumbers close to $k_{\rm tr}$, which compensates for the energy accumulation. This is reminiscent of condensates in 2D turbulence. Furthermore, we show that, when $k_{\rm tr}/k_f > 1$, the energy that accumulates near to $k_{\rm tr}$ generates a direct cascade of generalized enstrophy for $k_n > k_{\rm tr}$, whereas, when $k_{\rm tr}/k_f < 1$, the modes with $k_n < k_{\rm tr}$ are in statistical equilibrium.

Our modifications to the shell model with scale-dependent coefficients is not restricted to a given physical system [30]. Although the details of the dependence of the transitional scale may vary with the parameters of specific models, the energy-transfer mechanisms that we have identified are general, so they should appear in any turbulent system that has a 2D-like large-k dynamics and 3D-like small-k dynamics. Thus, our results will stimulate the study of new physical systems with such cascade arrests that lead to intermediate-scale condensates.

This work was supported in part by the French government through the UCA$^{\rm JEDI}$ Investments in the Future project managed by the National Research Agency (ANR), with reference number ANR-15-IDEX-01, and by the International Centre for Theoretical Sciences (ICTS) for the online program - Turbulence: Problems at the Interface of Mathematics and Physics (code: ICTS/TPIMP2020/12). KVK thanks Laboratoire J. A. Dieudonné of Université Côte d'Azur for hospitality. RP and KVK acknowledge support from SERB and NSM (India) and thank SERC (IISc) for computational resources. KVK is thankful to Siddhartha Mukherjee for useful discussions. DV acknowledges support from the International Centre for Theoretical Sciences (ICTS-TIFR), Bangalore, India.

[1] U. Frisch, Turbulence: The Legacy of A. N. Kolmogorov (Cambridge University Press, Cambridge, 1995).
[2] G. Boffetta and R. E. Ecke, Annu. Rev. Fluid Mech. **44**, 427 (2012).
[3] R. Pandit, D. Banerjee, A. Bhatnagar, M.-E. Brachet, A. Gupta, D. Mitra, P. P. N. Pal, S. Ray, V. Shukla, and D. Vincenzi, Phys. Fluids **29**, 111112 (2017).
[4] U. Frisch, A. Pomyalov, I. Procaccia, and S. S. Ray, Phys. Rev. Lett. **108**, 074501 (2012).
[5] A. Alexakis and L. Biferale, Phys. Rep. **767–769**, 1 (2018).
[6] M. Verma, Energy Transfers in Fluid Flows (Cambridge University Press, Cambridge, 2019).
[7] A. Pouquet, D. Rosenberg, J. E. Stawarz, and R. Marino, Earth and Space Science **6**, 351 (2019).
[8] A. van Kan, B. Favier, K. Julien, and E. Knobloch, J. Fluid Mech. **952**, R4 (2022).
[9] S. J. Benavides, K. J. Burns, B. Gallet, J. Y.-K. Cho, and G. R. Flierl, J. Fluid Mech. **935**, A1 (2022).
[10] M. Linkmann, G. Boffetta, M. C. Marchetti, and B. Eckhardt, Phys. Rev. Lett. **122**, 214503 (2019).
[11] N. B. Padhan, K. V. Kiran, and R. Pandit, "Novel turbulence and coarsening arrest in active-scalar fluids," Soft Matter, in press (2024), arXiv:2402.00961.
[12] X. M. de Wit, M. Fruchart, T. Khain, F. Toschi, and V. Vitelli, Nature **627**, 515 (2024).
[13] T. Bohr, M. H. Jensen, G. Paladin, and A. Vulpiani, Dynamical Systems Approach to Turbulence (Cambridge University Press, Cambridge, 1998).
[14] A. Basu, A. Sain, S. K. Dhar, and R. Pandit, Phys. Rev. Lett. **81**, 2687 (1998).
[15] L. Biferale, Annu. Rev. Fluid Mech. **35**, 441 (2003).
[16] F. Plunian, R. Stepanov, and P. Frick, Phys. Rep. **523**, 1 (2013).
[17] X. M. de Wit, G. Ortali, A. Corbetta, A. A. Mailybaev, L. Biferale, and F. Toschi, arXiv preprint arXiv:2402.02994 (2024).
[18] A. A. Mailybaev, Phys. Rev. Fluids **6**, L012601 (2021).

[19] L. Biferale, A. A. Mailybaev, and G. Parisi, Phys. Rev. E **95**, 043108 (2017).
[20] C. J. Miles and C. R. Doering, J. Nonlin. Sci. **28**, 2153 (2018).
[21] R. Benzi, I. Castaldi, F. Toschi, and J. Trampert, Phil. Trans. R. Soc. A **380**, 20210074 (2022).
[22] G. Boffetta, F. De Lillo, and S. Musacchio, Phys. Rev. E **83**, 066302 (2011).
[23] A. Celani, S. Musacchio, and D. Vincenzi, Phys. Rev. Lett. **104**, 184506 (2010).
[24] S. Musacchio and G. Boffetta, Phys. Fluids **29** (2017).
[25] V. S. L'vov, E. Podivilov, A. Pomyalov, I. Procaccia, and D. Vandembroucq, Phys. Rev. E **58**, 1811 (1998).
[26] T. Gilbert, V. S. L'vov, A. Pomyalov, and I. Procaccia, Phys. Rev. Lett. , 074501 (2002).
[27] D. Pisarenko, L. Biferale, D. Courvoisier, U. Frisch, and M. Vergassola, Phys. Fluids **5**, 2533 (1993).
[28] C.-k. Chan, D. Mitra, and A. Brandenburg, Phys. Rev. E **85**, 036315 (2012).
[29] We have checked that the contribution of hyper-friction to the formation of the energy condensate is negligible.
[30] A shell-model version of the 3D NSE with odd viscosity [12] could be constructed by adding a term proportional to $-\mathrm{i}k_n^2 u_n$ to the SABRA model, in the same spirit as shell models of rotating turbulence [31].
[31] S. K. Rathor, S. Chakraborty, and S. S. Ray, Phys. Rev. E **105**, L063102 (2022).